

Surfactant-Templated Organic Functionalized Mesoporous Silica with Phosphino Ligands

Qingyuan Hu,[†] J. Eric Hampsey,[†] Nan Jiang,[‡] Chaojun Li,[‡] and Yunfeng Lu^{*,†}

Department of Chemical and Biomolecular Engineering, Tulane University, New Orleans, Louisiana 70118, and Department of Chemistry, Tulane University, New Orleans, Louisiana 70118

Received May 19, 2004. Revised Manuscript Received November 28, 2004

Ordered organic functionalized mesoporous silica containing covalently bonded diphenylphosphinoethyl ligands was synthesized using a surfactant-templating approach. Briefly, hydrolysis and condensation reactions of tetraethyl orthosilicate (TEOS) and 2-(diphenylphosphino)ethyl triethoxysilane (PPETS) in an acidic condition produced phosphino-ligand containing organosilicate species. Subsequent co-assembly of the organosilicate species with surfactants led to the formation of ordered organic/inorganic nanocomposites. Selective surfactant removal by controlled thermal decomposition created organic functionalized mesoporous silica with diphenylphosphinoethyl ligands covalently bonded to the silica framework. Pore structures and pore sizes of the functionalized mesoporous silica were controlled by using different surfactants such as P123, F127, Brij-58, and CTAB. It was found that the added organosilane may significantly affect the mesostructure possibly through participating in the cooperative assembly process. These organic functionalized mesoporous silicas were bonded with palladium ions, resulting in the formation of catalytically active organometallic complexes that show excellent activities in both Heck and epoxides allylation reactions. Compared with the conventional homogeneous catalysts, these heterogeneous organometallic complexes can be readily separated from the reaction systems and reused without deteriorating their catalytic activities. This study provides a direct synthesis approach to efficiently synthesize a large variety of organic functionalized mesoporous silica with controlled pore sizes, pore surface chemistry, and pore structure for heterogeneous catalysts and other applications.

1. Introduction

Since their discovery in the early 1990s, surfactant-templated mesoporous materials with unique properties (e.g., high surface area, high pore volume, controlled pore structure, and uniform pore size distribution)^{1,2} are of great interest for adsorption, separation, sensing, catalysis, and other applications.^{3–7} A decade of research in this area establishes the precise control of mesostructure through manipulating the cooperative assembly of surfactants and inorganic species such as silicates. For example, mesoporous silica with highly ordered hexagonal, cubic, or lamellar mesostructures can be readily prepared using different

surfactants and surfactant concentrations. Similarly, pore diameter of the mesoporous silica is controllable from 2 to over 20 nm by tuning the sizes of surfactant–liquid–crystalline assemblies.^{8–10} Besides the mesostructural control, functionalization of mesoporous materials has also been a focus, since the functionalized organic groups may provide mesoporous materials with improved stability to compression,¹¹ better compatibility and more favorable interactions with other components such as polymers, improved hydrothermal stability,¹² decreased water adsorption,^{13,14} less agglomeration between particles,¹⁵ and the capability to graft new reactive complexes such as organometallic catalysts to the pore surface.^{16,17}

* To whom correspondence should be addressed. Phone: (504) 865-5827; fax: (504) 865-6744; e-mail: ylu@tulane.edu.

[†] Department of Chemical and Biomolecular Engineering.

[‡] Department of Chemistry.

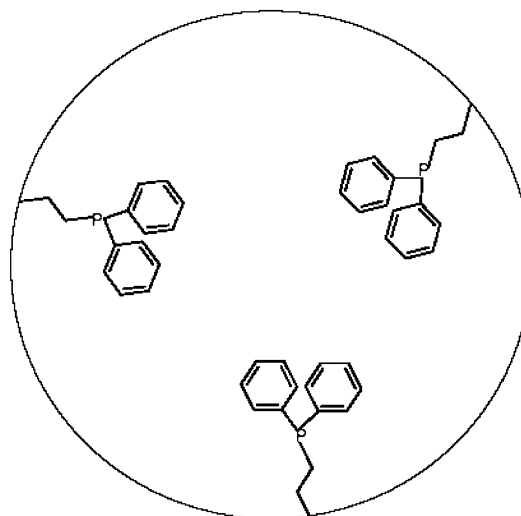
- (1) Kresge, C. T.; Leonowicz, M. E.; Roth, W. J.; Vartuli, J. C.; Beck, J. S. *Nature* **1992**, 359, 710–712.
- (2) Zhao, D.; Feng, J.; Huo, Q.; Melosh, N.; Frederickson, G. H.; Chmelka, B. F.; Stucky, G. D. *Science* **1998**, 279, 548–552.
- (3) Stein, A.; Melde, B. J.; Schrodin, R. C. *Adv. Mater.* **2000**, 12, 1403–1419.
- (4) Kosslick, H.; Mönlich, I.; Paetzold, E.; Fuhrmann, H.; Fricke, R.; Müller, D.; Oehme, G. *Microporous Mesoporous Mater.* **2001**, 44–45, 537–545.
- (5) Dams, M.; Drijkoningen, L.; Pauwels, B.; Van Tendeloo, G.; De Vos, D. E.; Jacobs, P. A. *J. Catal.* **2002**, 209, 225–236.
- (6) Tanaka, S.; Mizukami, F.; Niwa, S.; Toba, M.; Maeda, K.; Shimada, H.; Kunimori, K. *Appl. Catal., A: General* **2002**, 229, 165–174.
- (7) Lagasi, M.; Moggi, P. *J. Mol. Catal., A: Chem.* **2002**, 182–183, 61–72.

- (8) Alberius, P. C. A.; Frindell, K. L.; Hayward, R. C.; Kramer, E. J.; Stucky, G. D.; Chmelka, B. F. *Chem. Mater.* **2002**, 14, 3284–3294.
- (9) Lu, Y.; Ganguli, R.; Drewien, C. A.; Anderson, M. T.; Brinker, C. J.; Gong, W.; Guo, Y.; Soye, H.; Dunn, B.; Huang, M. H.; Zink, J. I. *Nature* **1998**, 389, 364–368.
- (10) Lu, Y.; Fan, H.; Stump, A.; Ward, T. L.; Rieker, T.; Brinker, C. J. *Nature* **1999**, 398, 223–226.
- (11) Koyano, K. A.; Tatsumi, T.; Tanaka, Y.; Nakata, S. *J. Phys. Chem. B* **1997**, 101, 9436–9440.
- (12) Van Der Voort, P.; Baltes, M.; Vansant, E. F. *J. Phys. Chem. B* **1999**, 103, 10102–10108.
- (13) Antochshuk, V.; Jaroniec, M. *Chem. Commun.* **1999**, 2373–2374.
- (14) Jaroniec, C. P.; Kruk, M.; Jaroniec, M.; Sayari, A. *J. Phys. Chem. B* **1998**, 102, 5503–5510.
- (15) Bourgeat-Lami, E. *Microspheres, Microcapsules Liposomes* **2002**, 5, 149–194.
- (16) Dý'az, J. F.; Balkus, K. J., Jr.; Bedioui, F.; Kurshev, V.; Kevan, L. *Chem. Mater.* **1997**, 9, 61–67.
- (17) Tudor, J.; O'Hare, D. *Chem. Commun.* **1997**, 603–604.

To date, organic moieties such as methyl, alkyl chains, vinyl, methacrylate, amino, thiol, sulfonic, phenyl, and metal/ligand complexes^{11,18–25} were functionalized onto the porous surface of mesoporous silica through so-called postsynthesis or direct-synthesis techniques. Postsynthesis modification technique is the most common method used to functionalize the mesoporous silica by attaching organic moieties to pore surface of preformed mesoporous silica through silylation reactions. In most cases, such surface modification reactions involve reactions of surface Si–OH groups with organosilane molecules such as $R_n\text{--SiX}_{4-n}$, where X represents an alkoxide or halide group and R is a non-hydrolyzable functional group such as an alkyl, vinyl ($-\text{CH}=\text{CH}_2$), thiol ($-(\text{CH}_2)_3\text{SH}$), amine ($-\text{NH}_2$ or $-\text{NR}_2$), and thianthrene. The density of functional groups attached on the pore surface is dependent on the density of the surface Si–OH groups, pore accessibility, and effectiveness of the silylation reactions. The direct-synthesis approach involves co-condensation of silicate species and organosilicates that contain non-hydrolyzable functional ligands in the presence of templating surfactant molecules. During the co-assembly process, organosilicates that contain hydrophobic ligands may serve as cosurfactants and insert the ligands into the hydrophobic micellar cores, resulting in a preferred ligand distribution along the silicate/surfactant interface. Subsequent surfactant removal leads to the formation of organic functionalized mesoporous materials with organic ligands covalently bonded on the pore surface. This approach has led to many organic functionalized mesoporous silica materials with various surface functional groups, such as fluorinated alkane-, mercapto-, phosphino-, and amino-functionalized organosilanes, thiol, sulfonic surface groups ($-\text{SO}_3\text{H}$), straight-chain alkanes, and methacrylate groups ($\text{CH}_2=\text{C}(\text{CH}_3)\text{CO}_2-$).^{26–32}

This research focuses on a direct synthesis of organic functionalized mesoporous silica containing active phosphino ligands that can form a large variety of stable, catalytically active organometallic complexes. Different surfactants including cationic hexadecyltrimethylammonium bromide

Scheme 1. Schematic of the Organic Functionalized Silica with a Covalently Bonded Diphenylphosphinoethyl Ligand



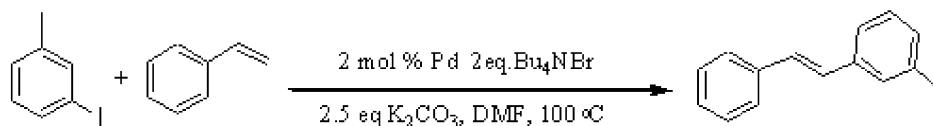
(CTAB), nonionic Brij-58, and triblock copolymer Pluronic P123 and F127 were used to template the pore structure. A model functionalizing organosilane 2-(diphenylphosphino)ethyl triethoxysilane (PPETS) was then used to provide covalently bonded phosphino ligands on the pore surface. Refluxing the organic functionalized mesoporous silica with palladium ions in a solution results in the formation of active palladium complexes catalytically active for Heck and epoxides allylation reactions. We hypothesized that, through controlling co-assembly of the silicates and the surfactants, the pore diameter of the active complexes can be precisely controlled, while mesostructures can also be controlled from two-dimensional hexagonal, three-dimensional bicontinued cubic, to the disordered mesostructure. Such tunable pore size and pore structure in turn should affect mass transportation and the catalytic activities of the complexes. This research provides an efficient direct synthesis approach toward organic-functionalized, controlled-structured, mesoporous silica that is of great importance for heterogeneous catalysts and other applications.

2. Experimental Section

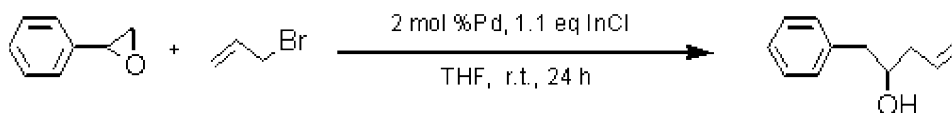
2.1 Formation of Organic Functionalized Mesoporous Silica. Mesoporous silica xerogels functionalized with diphenylphosphinoethyl groups were prepared using a sol–gel surfactant-templating approach. Block copolymer surfactant Pluronic P123 ($\text{EO}_{20}\text{PO}_{70}\text{EO}_{20}$) and F127 ($\text{EO}_{106}\text{PO}_{70}\text{EO}_{106}$) (from BASF, EO and PO, respectively, designate poly(ethylene oxide) and poly(propylene oxide)), cationic surfactant CTAB (hexadecyltrimethylammonium bromide) (Aldrich), and nonionic surfactant Brij-58 ($\text{C}_{16}\text{H}_{33}(\text{OCH}_2\text{CH}_2)_{20}\text{OH}$) (Aldrich) were used as the pore structure-directing agents. Tetraethyl orthosilicate (TEOS) (reagent grade 98%, Aldrich), 2-(diphenylphosphino)ethyltriethoxysilane (PPETS) (95%, Gelest), ethanol (200 proof (absolute), Aldrich), HCl (ACS reagent 37%, Aldrich), and deionized water (18 M Ω) were used as received. Typical precursor sols were prepared by mixing these chemicals in molar ratios of TEOS:ethanol:HCl:water:surfactant:PPETS = 1:38:0.01:5:0.01–0.25:0.05–0.20. The mixtures were sonicated for 30 min at room temperature and then cast in Petri dishes and dried at room temperature for 3 days to obtain xerogels. The xerogels were then calcined at 350 °C under N_2 for 4 h or extracted using

- (18) Shimojima, A.; Kuroda, K. *Langmuir* **2002**, *18*, 1144–1149.
- (19) Moller, K.; Bein, T.; Fischer, R. X. *Chem. Mater.* **1999**, *11*, 665–673.
- (20) Van Rhijn, W. M.; De Vos, D. E.; Sels, B. F.; Bossaert, W. D.; Jacobs, P. A. *Chem. Commun.* **1998**, 317–318.
- (21) Liu, J.; Feng, X.; Fryxell, G. E.; Wang, L. Q.; Kim, A. Y.; Gong, M. *Adv. Mater.* **1998**, *10*, 161–165.
- (22) Feng, X.; Fryxell, G. E.; Wang, L. Q.; Kim, A. Y.; Liu, J.; Kemner, K. M. *Science* **1997**, *276*, 923–926.
- (23) Lim, M. H.; Blanford, C. F.; Stein, A. *Chem. Mater.* **1998**, *10*, 467–470.
- (24) Burkett, S. L.; Sims, S. D.; Mann, S. *Chem. Commun.* **1996**, 1367–1368.
- (25) Rao, Y. V. S.; De Vos, D. E.; Bein, T.; Jacobs, P. A. *Chem. Commun.* **1997**, 355–356.
- (26) Fan, H.; Lu, Y.; Stump, A.; Reed, S. T.; Baer, T.; Schunk, R.; Perez-Luna, V.; Lopez, G. P.; Brinker, C. J. *Nature* **2000**, *405*, 56–60.
- (27) Sims, S. D.; Burkett, S. L.; Mann, S. *Mater. Res. Soc. Symp. Proc.* **1996**, *431*, 77–82.
- (28) Lim, M. H.; Blanford, C. F.; Stein, A. *J. Am. Chem. Soc.* **1997**, *119*, 4090–4091.
- (29) Yokoi, T.; Yoshitake, H.; Tatsumi, T. *Chem. Mater.* **2003**, *15*(24), 4536–4538.
- (30) Walcarius, A.; Delacote, C. *Chem. Mater.* **2003**, *15*(22), 4181–4192.
- (31) Liu, C.; Naismith, N.; Fu, L.; Economy, J. *Chem. Commun. (Cambridge)* **2003**, *15*, 1920–1921.
- (32) Bitterwolf, T. E.; Newell, J. D.; Carver, C. T.; Addleman, R. S.; Linehan, J. C.; Fryxell, G. *Inorgan. Chim. Acta* **2004**, *357*, 3001–3006.

Scheme 2. Scheme of the Heck Reaction of 3-Iodotoluene and Styrene



Scheme 3. Scheme of Allylation Reaction of Allyl Bromide and Styrene Oxide



ethanol to remove the surfactants. The complete removal of the surfactant was confirmed by TGA, nitrogen adsorption, and other techniques. The structure of the functionalized silica xerogels is schematically shown in the Scheme 1. The formation of palladium complexes was achieved by refluxing the functionalized mesoporous silica in a palladium acetate *N,N*-dimethylformamide (DMF) (ACS reagent >99.8%, Aldrich) solution under nitrogen for 12 h. The solid products were collected by filtration, washed with DMF to remove the uncomplexed palladium, dried at room temperature, and then treated in hydrogen for 12 h at 150 °C.

2.2 Characterization. Thermogravimetric analyses (TGA) were carried out using a Hi-Res TGA 2950 Thermogravimetric Analyzer (TA Instruments) using a nitrogen flow of 80 mL/min and a heating rate of 5 °C/min. Infrared pellets of the samples were recorded on a NEXUS 670 FT-IR spectrometer (Thermo Nicolet Co.) with a resolution of 4 cm⁻¹. The infrared pellets were prepared using the conventional KBr pressing method. Nitrogen adsorption and desorption isotherms were obtained using a Micromeritics ASAP 2010. The BET surface area and pore size distribution³³ were calculated from the isotherms using the ASAP 2010 v.5 software. X-ray diffraction (XRD) measurements were performed on a Philips Xpert X-ray diffractometer using Cu K α radiation. Transmission electron microscope (TEM) micrographs were obtained using a JEOL 2010 microscope operated at 120 KV. GC/MS data were obtained by HP 5890 Series II gas chromatography and HP5989A mass spectrometer. Flash chromatography employed Kiesegel 60, 230–400 mesh purchased from Sorbent Technologies.

2.3 Catalysis Test. Heck reaction^{34–36} and allylation of aldehydes are important synthetic organic reactions.^{37–39,49} In this research, a

Heck reaction of 3-iodotoluene and styrene (see Scheme 2) and the allylation reactions (see Scheme 3) were used to examine the catalytic activity of the mesoporous silica-supported organo–palladium complexes.

In a typical Heck reaction, styrene (0.5 mmol, 1 equiv), 3-iodotoluene (0.5 mmol, 1 equiv), and the palladium catalyst (0.01 mmol, 0.02 equiv) were added into a well-stirred suspension containing K₂CO₃ (1.25 mmol, 2.5 equiv), *n*-tetrabutylammonium bromide (1.00 mmol, 2 equiv), and 2 mL DMF (containing 2% H₂O) in air. The palladium catalysts were prepared by binding palladium acetate with the organic functionalized mesoporous silica prepared with 5% of PPETS. The mixture was sealed and heated at 373 K for 24 h for a complete reaction. After cooling, 5 mL EtOAc was added to the reaction mixture. The catalyst was recovered by filtration and reused at least three times. The organic phase was dried using MgSO₄ and purified by flash chromatography.

In a typical allylation reaction, the molar ratio of InCl/allyl bromide/styrene oxide was kept at 2.2/2.0/1.0. The amount of palladium catalysts used was 2 mol-% of the styrene oxide precursor. After stirring for 24 h, the crude products were purified by flash chromatography. The catalysts were recovered under nitrogen to prevent oxidation and were reused three times. The details of purification and characterization of products were described in our previous paper.⁴⁹

3. Results and Discussion

3.1 Formation of Organic Functionalized Mesoporous Silica by Selective Surfactant Removal. This research uses PPETS and TEOS as the silica sources. Each PPETS molecule contains a non-hydrolyzable hydrophobic diphenylphosphinoethyl (DPPE) ligand and three hydrolyzable ethoxy groups. Hydrolysis and condensation reactions of PPETS and TEOS result in organosilicate clusters. Co-assembly of surfactants and the organosilicates forms ordered surfactant/silicate nanocomposites containing the DPPE ligands. Selective surfactant removal results in the formation of functionalized mesoporous silica with the DPPE ligands covalently attached on the pore surface. In this study, a suitable calcination condition has been developed to selectively decompose the surfactants while maintaining the active DPPE ligands covalently bonded on the pore surface.

The selective decomposition process was demonstrated by TGA and FTIR techniques using the P123-templated func-

- (33) Brunauer, S. P.; Emmett, H.; Teller, E. *J. Am. Chem. Soc.* **1938**, *60*, 309–319.
- (34) Bhanage, B. M.; Shirai, M.; Arai, M. *J. Mol. Catal., A: Chem.* **1999**, *145*, 69–74.
- (35) Anson, M. S.; Mirza, A. R.; Tonks, L.; Williams, J. M. J. *Tetrahedron Lett.* **1999**, *40*, 7147–7150.
- (36) Mingzhong, C.; Jun, Z.; Hong, Z.; Caisheng, S. *React. Funct. Polym.* **2002**, *50*, 191–195.
- (37) Negishi, E. I.; Liou, S. T. In *Handbook of Organopalladium Chemistry for Organic Synthesis*; Negishi, E. I., Ed.; John Wiley & Sons: 2002; Vol. 2, pp 1769–1793.
- (38) Thadani, A. N.; Batey, R. A. *Org. Lett.* **2002**, *4*, 3827.
- (39) Nokami, J.; Anthony, L.; Sumida, S. I. *Chem. Eur. J.* **2000**, *2*, 847.
- (40) Dolphin, D.; Wick, A. *Tabulation of Infrared Spectral Data*; John Wiley & Sons, Inc., 1977.
- (41) Bentley, F. F.; Smithson, L. D.; Rozek, A. L. *Infrared Spectra and Characteristic Frequencies*; John Wiley & Sons, Inc., 1968.
- (42) Lin-Vien, D.; Colthup, N. B.; Fateley, W. G.; Grasselli, J. G. *The Handbook of Infrared and Raman Characteristic Frequencies of Organic Molecules*.
- (43) Socrates, G. *Infrared Characteristic Group Frequencies*; John Wiley & Sons, Inc., 1994.
- (44) Liu, X.; Tian, B.; Yu, C.; Gao, F.; Xie, S.; Tu, B.; Che, R.; Peng, L.-M.; Zhao, D. *Angew. Chem., Int. Ed.* **2002**, *41*(20), 3876–3878.
- (45) Pyye, G.; Sjöblom, J.; Stöcker, M. *Adv. Colloid Interface Sci.* **2001**, *89–90*, 439–466.
- (46) Wang, S. W.; Sun, Y.; Zhong, B. *Mater. Res. Bull.* **2001**, *36*, 1717–1720.

- (47) Kosslick, H.; Lischke, G.; Landmesser, H.; Parltitz, B.; Storek, W.; Fricke, R. *J. Catal.* **1998**, *176*, 102–114.
- (48) Gregg, S. J.; Sing, K. S. W. *Adsorption, surface area and porosity*; Academic Press: 1992.
- (49) Jiang, N.; Hu, Q.; Reid, C. S.; Lu, Y.; Li, C.-J. *Chem. Commun.* **2003**, 2318–2319.

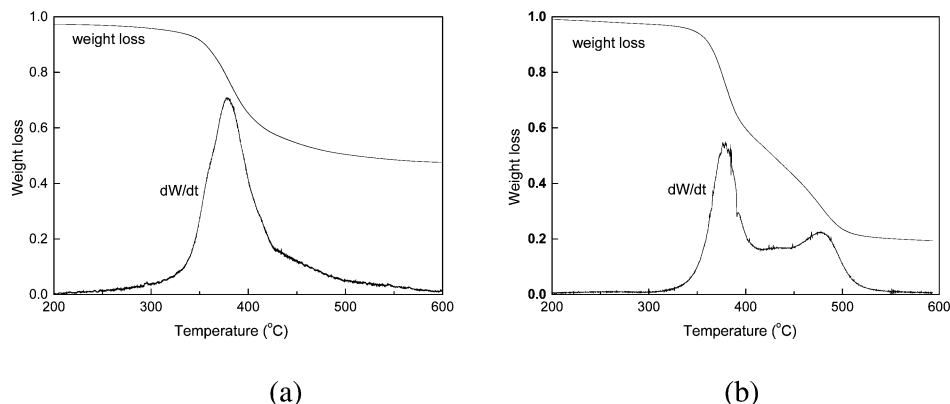


Figure 1. TGA curves of silica xerogels prepared with (a) TEOS as the silica source and (b) TEOS and PPETS as the silica source.

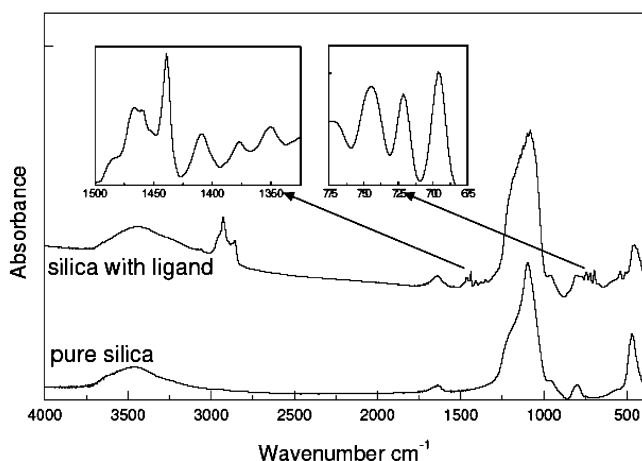


Figure 2. FT-IR spectra of the calcined silica xerogels prepared with 20% PPETS and pure mesoporous silica prepared with 0% PPETS under the same condition.

tionalized silica as a model system. Figure 1a shows TGA curve of a silica/surfactant xerogel prepared using TEOS as the only silica source. Under a nitrogen atmosphere, the TGA curve indicates that the decomposition of the surfactant starts at about 250 °C with a single weight loss peak centered at approximately 380 °C. The weight loss (52.9%) obtained from the TGA curve is consistent with the amount of the surfactant added (55%), indicating that the surfactant can be almost completely removed using the decomposition approach. Figure 1b shows a TGA curve of a silica/surfactant xerogel prepared using TEOS and 20 mol-% PPETS as the silica source. Two weight loss peaks can be clearly visible at 380 and 490 °C, respectively. Comparison of the TGA curves in Figure 1a and b suggests that the first decomposition peak centered at 380 °C is attributed from the decomposition of the P123 surfactant while the second peak centered at 490 °C comes from the decomposition of the phosphino ligand. The first and the second weight lost are, respectively, around 47% and 21%, which is also consistent with the amounts of surfactant (47%) and ligand (19%) added to the nanocomposites. These results suggest that a controlled calcination process under nitrogen at a temperature between 300 and 400 °C should remove the surfactant while preserve the DPPE ligands.

The retention of the DPPE ligand is further confirmed by the FTIR spectroscopic study. Figure 2 shows the FTIR spectra of the organic functionalized mesoporous silica

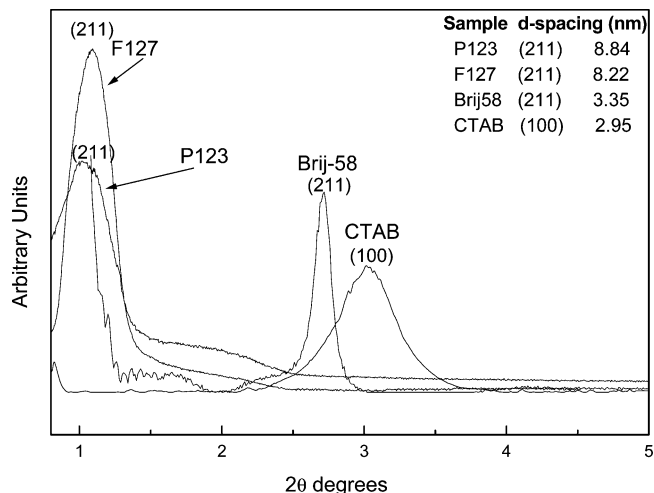


Figure 3. Low-angle XRD patterns of the organic functionalized mesoporous silica prepared with 5% of PPETS and different surfactant templates.

prepared with 20 mol-% of PPETS and pure mesoporous silica calcined under the same condition. The strong stretching bands at 2923 cm^{-1} and 2853 cm^{-1} are attributed to the asymmetric and symmetric stretching modes of C–H bonds. The weak absorbance at 1460 and 720 cm^{-1} can be, respectively, assigned to the methylene scissoring mode and the rocking mode of the $-(\text{CH}_2)-$ moieties;^{40,43} the bands at 750 and 1100 cm^{-1} are due to the asymmetric Si–C stretching mode and the Si–O stretching vibration mode, respectively. The small absorption peaks around 3100 cm^{-1} and 690 cm^{-1} are, respectively, attributed to the stretching vibrations of the C–H bonds in the benzene rings and the C–H out-of-plane deformation of the monosubstituted benzene rings. The absorbance around 1470 cm^{-1} is due to the skeletal vibrations of the benzene nucleus.³⁰ The absorbance at about 1435 cm^{-1} is attributed to the vibrations of P–CH₂. The absorbance of P-phenyl (1130–1090 cm^{-1}) is overlapped with the intense Si–O bonds at 1100 cm^{-1} and cannot be differentiated in this experiment.^{42,43} The samples prepared using a solvent extraction technique also show the similar FTIR spectrum (data not shown). Comparison of the FTIR spectrum between the mesoporous silica prepared with and without PPETS clearly indicates the retention of the DPPE ligand after surfactant removal. Combination of the TGA and FTIR studies suggests that it is possible to selectively remove the surfactant while retaining the organic

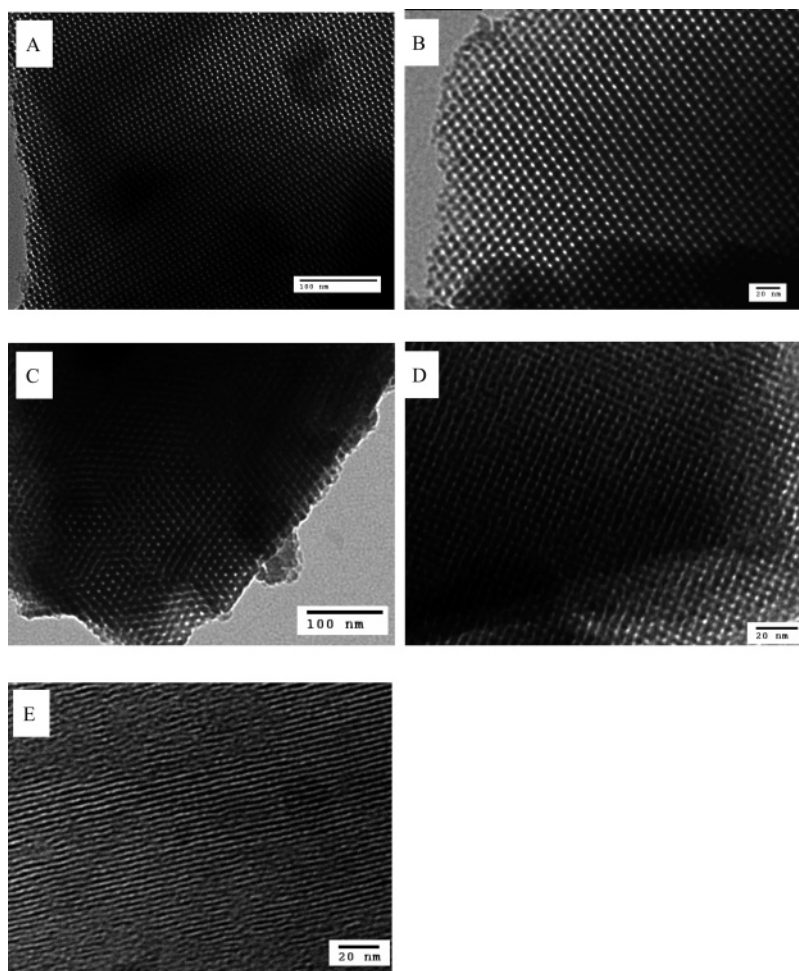


Figure 4. TEM images of the organic functionalized silica prepared with 5% PPETS and P123 (a [311] plane, b [110] plane), F127 (c), Brij 58 (d), and CTAB (e) as surfactant templates.

functional group using a controlled thermal decomposition approach.

3.2 Control Mesostructure by Using Different Surfactant Templates. To control pore structure and pore size of the organic functionalized mesoporous silica, different surfactants including P123, F127, Brij-58, and CTAB were used. Figure 3 shows the low-angle XRD patterns of the functionalized mesoporous silica prepared with 5% PPETS. The P123-templated sample shows an intense reflection at a d spacing of 8.84 nm. Combined with the TEM result shown in Figure 4, this diffraction peak can be indexed as the (211) reflection of a three-dimensional mesoporous $Ia3d$ mesostructure.⁴⁴ The F127-templated sample shows a diffraction peak at the d spacing of 8.22 nm, which can be indexed as the (211) reflection of a cubic mesostructure with a unit cell parameter of 20.2 nm. The Brij 58-templated sample shows a diffraction peak at the d spacing of 3.35 nm, which can be indexed as the (211) reflection of a cubic mesostructure with unit cell parameter of 8.2 nm. The CTAB-templated sample shows a diffraction peak at the d spacing of 2.95 nm, which can be indexed as the (100) reflection of a two-dimensional hexagonal mesostructure. Figure 4 shows the corresponding TEM images of the functionalized silica prepared with 5% PPETS. The P123-templated functionalized silica shows a highly ordered mesostructure along the [311] and [111] planes of an $Ia3d$ mesostructure.⁴⁴ TEM images of the F127-

templated and Brij-58 templated samples also show ordered mesostructures along their cubic [100] planes. The estimated unit cell parameter is, respectively, around 21.1 and 8.4 nm, which is consistent with the XRD result shown in Figure 3. The CTAB-templated sample shows an ordered pore structure with a pore-to-pore distance of 3.0 nm, which is also consistent with its XRD result.

The pore structure of these samples was further characterized using the nitrogen sorption experiments. As-synthesized silicate/surfactant composites prior to the surfactant removal are dense to nitrogen at 77 K. Removal of the surfactants results in functionalized mesoporous silica with controlled pore sizes and pore structures. Figure 5 and Figure 6, respectively, display the nitrogen adsorption/desorption isotherms and pore size distributions of the functionalized mesoporous silica prepared with 5% PPETS. The CTAB and Brij-58 templated samples show typical isotherms of the surfactant-templated mesoporous silica. The absence of hysteresis loops and of significant nitrogen uptakes at relative pressure higher than 0.4 indicate narrow pore size distributions.⁴⁸ The P123- and F127-templated functionalized mesoporous silicas show isotherms similar to those of unfunctionalized mesoporous silicas prepared with the same surfactants. The BET surface areas, average pore sizes, and pore volumes of these functionalized mesoporous silicas are summarized in Table 1.

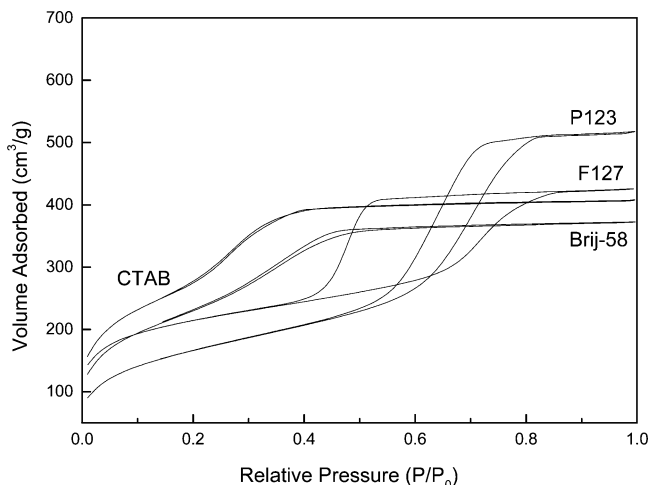


Figure 5. Nitrogen adsorption/desorption isotherms of the organic functionalized mesoporous silica prepared with different surfactants.

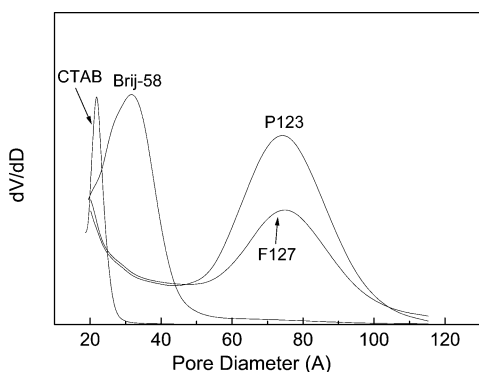


Figure 6. Pore size distributions of the organic functionalized mesoporous silica prepared with different surfactants.

Table 1. Surface Areas, Pore Diameters, and Pore Volumes of Organic Functionalized Mesoporous Silica Templated by Different Surfactants with Varying Amounts of Ligand

samples	ligand content	BET surface area (m ² /g)	average pore size (Å)	pore volume (cm ³ /g)
P123-templated	0	671 ± 2	79	0.90
	5%	640 ± 2	72	0.80
	10%	604 ± 2	66	0.79
	20%	504 ± 1	60	0.72
F127-templated	5%	553 ± 2	71	0.58
Brij 58-templated	5%	643 ± 11	32	0.58
CTAB-templated	5%	987 ± 8	25	0.63

3.3 Effects of the DPPE Concentration. The above XRD, TEM, and nitrogen sorption studies suggest a possibility of controlling mesostructure by using different surfactants as templates. It is also important to understand the role of the PPETS organosilane during the co-assembly process and its concentration effect on the pore structure. Generally, the mesostructure of silicate/surfactant assemblies can be described using a classical micellar packing parameter, $P = v/(a_0 l_c)$, where a_0 is the cross-sectional hydrophilic headgroup area, v is the tail volume, and l_c is the length of hydrophobic tail.^{50,51} An increase of P from $1/3$ to 1 may continuously transform the mesostructure from spherical micelles to lamellar structure. Although this simple hydrophilic–

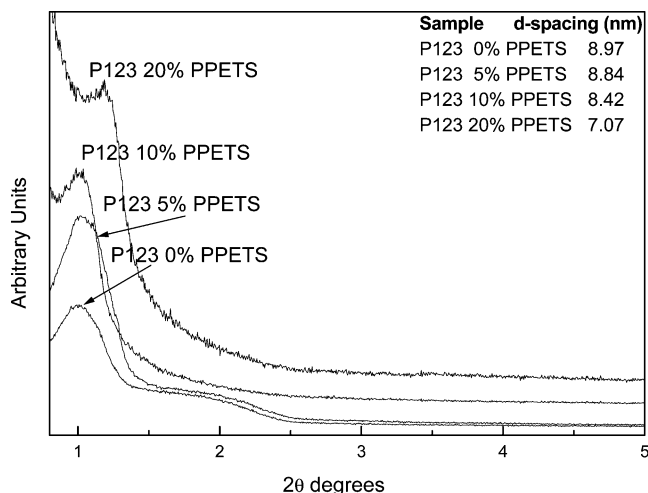


Figure 7. Low-angle XRD patterns of P123-templated organic functionalized mesoporous silica prepared with 0–20% PPETS.

hydrophobic balance-based model cannot fully describe the complexity of the self-assembly process (for example, surfactant concentration, temperature, solvent, and external fields may dramatically affect the final assembled mesostructure), it provides a basic understand of the self-assembling system. According to this model, many new mesostructures have been synthesized by adjusting the packing parameter P through mixing surfactants or block copolymers, as well as other approaches.^{52–54} Since each PPETS molecule contains a non-hydrolyzable hydrophobic ligand, hydrolysis of the PPETS molecules generates amphiphilic organosilicates that contain hydrophilic silanol groups (SiOH) and the hydrophobic 2-(diphenylphosphino)-ethyl ligands. Such amphiphilic organosilicates may serve as cosurfactants and are preferably located along the hydrophilic/hydrophobic interfaces. These amphiphilic organosilicates contain bulky diphenylphosphinoethyl ligands and oligomeric silanol groups (after condensation reactions). According to this model, the participation of these bulky amphiphilic species in the surfactant/silicates co-assembly may result in a larger packing parameter, increase the mesostructure curvature, and in turn affect the final mesostructures.

Figure 7 shows the low-angle XRD patterns of the P123-templated mesoporous silica prepared with 0, 5, 10, and 20% PPETS. When the concentration of PPETS was increased to 5%, the primary diffraction peak slightly shifts toward a smaller d -space value, from 9.0 nm (0%) to 8.84 nm (5%) with an additional peak presented at 1.35° of 2θ . Since it is unlikely to determine the pore symmetry from this XRD diffraction, TEM is used to confirm the mesostructure. Figure 8 shows the TEM images of the mesoporous silica prepared with 0% PPETS, indicating a highly ordered [100] orientation of a 2D hexagonal mesostructure with a center-to-center pore distance of 8.8 nm. Combined with the TEM result, the intense XRD diffraction peaks of the mesoporous silica (0%

(50) Huo, Q.; Leon, R.; Petroff, P. M.; Stucky, G. D. *Science* **1995**, 268, 1324.

(51) Huo, Q.; Margolese, D.; Stucky, G. D. *Chem. Mater.* **1996**, 8, 1147.

(52) Kim, J. M.; Park, S.-E.; Stucky, G. D. 13th International Zeolite Conference, Montpellier, France, July 8–13, 2001.

(53) Ryoo, R.; Joo, S.-H.; Kim, J.-M. *J. Phys. Chem. B* **1999**, 103, 7435–7440.

(54) Ryoo, R.; Ko, C.-H.; Park, I.-S. *Chem. Commun.* **1999**, 1413–1414.

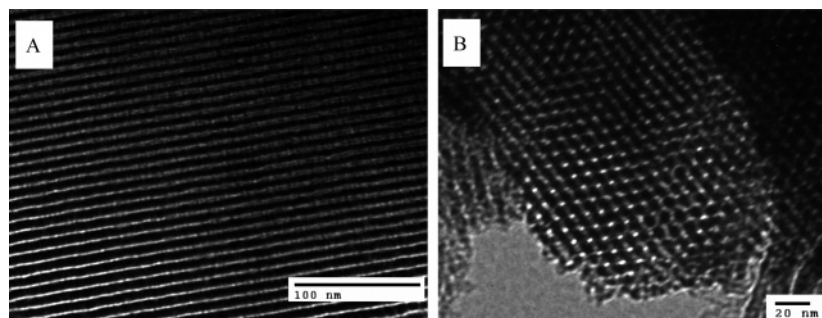


Figure 8. TEM images of P123-templated mesoporous silica prepared with TEOS as the only silica source (a [100] plane, b [110] plane).

PPETS) at the d spacing of 8.97 nm (2θ of 0.98°) and 4.40 nm (2θ of 2.0°) can be, respectively, indexed as the (100) and (200) reflections of a 2D hexagonal mesostructure. Compared to the mesostructure of the functionalized silica prepared with 5% PPETS (see TEM images in Figure 4 and the XRD results in Figure 3 and Figure 7), a mesophase transformation from hexagonal to $Ia3d$ cubic is revealed. Such a mesophase transformation may result from the participation of the amphiphilic organosilicates in the co-assembly discussed above. However, further increasing the organic ligand concentration may decrease the efficiency of co-assembly, leading to a deteriorated long-range ordering as indicated by the disappearance of second-order XRD diffraction and the weakening of the diffraction intensity.

Compared with a hexagonal pore system, a bicontinuous $Ia3d$ cubic mesostructure has many advantages in catalytic and many other applications, since the bicontinuous three-dimensional pore system may prevent pore blockage^{33–36} and promote a more agitated flow, which can enhance the interactions between reactants and the catalytic sites. However, our experiments showed that the $Ia3d$ cubic structure is formed only in a very narrow window. The use of a lower PPETS content (e.g., <3%) often results in mixed hexagonal and cubic mesostructure, while a high PPETS content (e.g., >10%) results in less ordered mesostructures. More comprehensive study is underway to understand the organic ligand effects in different surfactant-templating systems.

Figure 9 and Figure 10 show the nitrogen adsorption/desorption isotherms and pore size distributions of the P123-templated functionalized mesoporous silica prepared with 0–20% of PPETS. All these samples show high surface area, large pore size, and pore volume (see Table 1). However, an increase of the PPETS content leads to the decreases in pore size, pore volume, and surface area. Two possible reasons may have contributed to this phenomenon. Since each PPETS molecule contains only three reactive ethoxy groups compared with four groups in a TEOS molecule, an increased PPETS concentration may weaken the silicate framework modulus and promote collapse or shrinkage of silicate framework upon the removal of the surfactant templates. This in turn produces mesoporous materials with smaller pore sizes and less ordered pore structure. Also, the presence of the organic ligand on the pore surface may have contributed to the decreased pore sizes and pore volume.

3.4 Palladium Binding and Catalytic Activity. Activity of the covalently bonded DPPE ligands was evaluated through the formation of catalytically active palladium

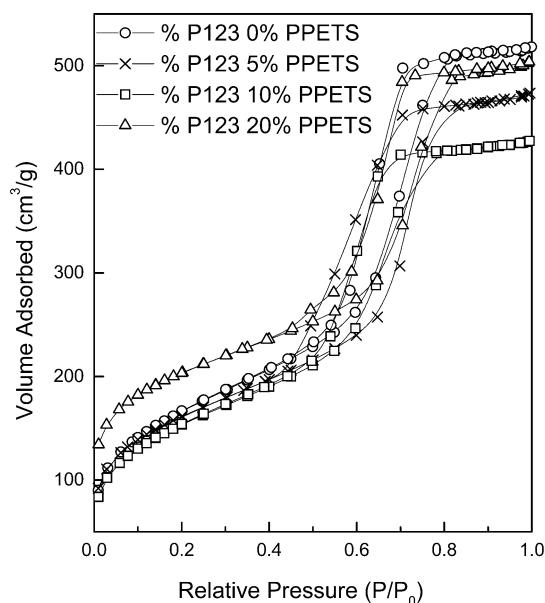


Figure 9. Nitrogen adsorption/desorption isotherms of the functionalized mesoporous silica prepared with 0–20% PPETS.

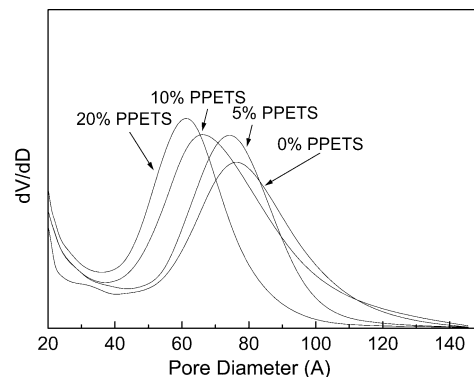


Figure 10. The effects of PPETS content on the pore size distributions of the functionalized mesoporous silica.

complexes. Figure 11 shows the TEM micrographs of the functionalized mesoporous silica after the palladium binding, indicating the preserved ordered mesostructures after the complexation process (see Figure 4). Besides the formation of organometallic complexes, palladium nanoparticles with diameters less than 10 nm were also observed, which may be due to the aggregation of palladium clusters or atoms during the hydrogen treating process. Detailed research is underway to characterize chemical nature of the catalytic sites, which will be discussed elsewhere.

The Heck reaction of 3-iodotoluene and styrene was conducted using the palladium-bonded P123-templated func-

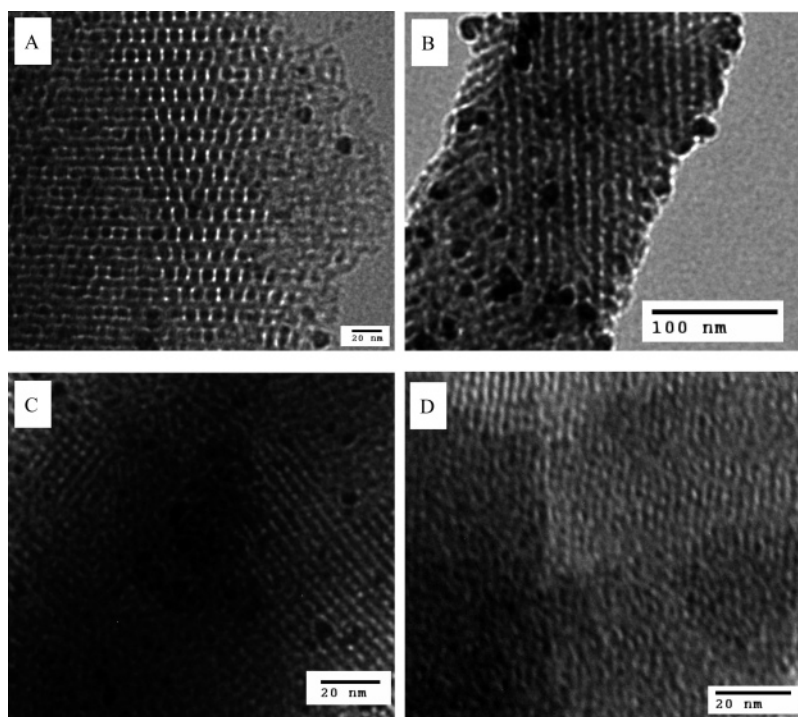
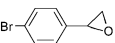
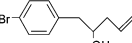
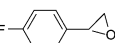
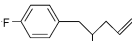
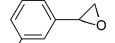
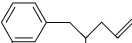
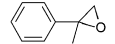
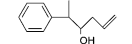
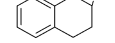
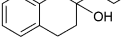
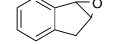
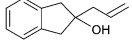
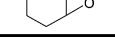
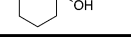


Figure 11. TEM micrographs of the functionalized mesoporous silica prepared with 5% PPETS and P123 (a), F127 (b), Brij 58 (c), and CTAB (d) as surfactant templates after the palladium binding and hydrogen treating.

Table 2. Allylation of Various Epoxides by the P123 Templated Organometallic Catalyst

Epoxide	Produces	Yield (%)
		62
		76
		69
		58
		71
		83
		47

functionalized mesoporous silica prepared with 5% PPETS as a catalyst. This catalyst gives a high conversion of 87%, which is comparable to that of commercial homogeneous $\text{Pd}(\text{PPh}_3)_4$ catalyst. We further examined its catalytic activity for various epoxide allylation reactions shown in Table 2. All the styrene-oxide derivatives, including the 2-methyl styrene oxide and the cyclic epoxides, gave target products with high yields, indicating that the heterogeneous catalyst is highly effective for the epoxide allylation reactions. The palladium-bonded functionalized silica can be readily recovered by filtration and reused without significantly deteriorating their catalytic activity. For example, the P123-templated catalyst was recovered and reused four times and, respectively,

Table 3. The Effect of Pore Structure on Conversion and Yield of Styrene Oxide Allylation Reactions

catalysts	conversion (%)	yield (%)
P123-templated	85	74
F127-templated	82	66
Brij 58-templated	66	53
CTAB-templated	29	15

showed a high conversion of 87%, 82%, 85%, and 83% in the Heck reaction. Similarly, it was recovered and reused three times and, respectively, showed a conversion of 83%, 82%, and 82% for the epoxide allylation. Control epoxide allylation studies conducted in identical conditions using homogeneous $\text{Pd}(\text{PPh}_3)_4$ as catalyst resulted in a comparable 82% conversion. However, these homogeneous catalysts cannot be easily recovered and reused. These reactions are demonstrated here to illustrate the formation of active organic functionalized mesoporous silica and active organometallic complexes rather than a systematic catalytic study.

3.5 Effect of Pore Structure on Catalytic Activity. The allylation reactions were conducted using the functionalized mesoporous silica with different pore sizes and pore structures. Table 3 summarizes the reaction conversions and yields using the catalysts templated by P123, F127, Brij-58, and CTAB. As shown in Table 1, these catalysts possess different pore structures and pore diameters ranging from 2.4 to 7.2 nm. The P123- and F127-templated catalysts contain similar pore diameters (7.2 nm), surface areas (640 m^2/g and 553 m^2/g), and cubic mesophase symmetry. As expected, similar conversions of 85% and 82% and similar yields of 70% and 66% were obtained for P123- and F127-templated catalysts, respectively. The slightly higher conversion and yield resulting from the P123-templated catalyst may be attributed to the higher pore volume (0.8 cm^3/g vs 0.58 cm^3/g), higher surface area, and bicontinuous pore channel. The Brij58-templated catalyst, which contains a three-dimensional cubic

mesostructure, a higher surface area ($643 \text{ m}^2/\text{g}$), and a comparable pore volume ($0.575 \text{ cm}^3/\text{g}$) but a smaller pore diameter (3.2 nm), gives a lower conversion (66%) and yield (53%). The CTAB-templated catalyst, which contains two-dimensional hexagonal porous networks, a highest surface area ($987 \text{ m}^2/\text{g}$), a large pore volume ($0.628 \text{ cm}^3/\text{g}$), but a smallest pore diameter (2.4 nm), gives a lowest conversion (29%) and yield (15%). Comparison of these results suggests that pore size has a more significant effect on the catalytic activities. The low conversion and yield resulting from the catalysts with smaller pore sizes may arise from the difficulties of forming π -allylpalladium(II) complexes within the narrow pore networks or from the increased diffusion resistance within the narrower pore channels. Larger pore size and the more openness of the structure to the environment (e.g., cubic vs hexagonal) favors efficiency of diffusion and contact to the catalytic sites.

4. Conclusions

We have demonstrated the formation of functionalized mesoporous silica with controllable pore structure and with active DPPE ligands covalently attached to the silica framework using a simple one-step surfactant-templating approach. Co-assembly of the ligand-containing organosilicates with surfactants followed by a selective surfactant removal results in organic functionalized mesoporous silica

with precise mesostructure control. The addition of the DPPE ligand not only provides the binding sites for metal ions but also influences the mesostructure formation, which confirmed that the hydrophilic–hydrophobic balance model can be used to direct the synthesis of mesoporous silica with controlled pore structures. An increased ligand concentration gradually changes the mesostructure from hexagonal, to $Ia3d$ cubic, and to a disordered mesostructure when the surfactant P123 is used.

These organic functionalized mesoporous silica can effectively bind with palladium and form highly active organometallic catalysts for Heck and allylation reactions. Tuning the pore sizes and pore structures of these catalysts in turn allows controlling their catalytic activity. A pore structure with opened pore channels, large enough pore diameter, and high surface should favor a higher catalytic activity. This research provides an efficient approach to synthesize heterogeneous catalysts with good catalytic activity and reusability for many potential industry applications.

Acknowledgment. This work is financially supported by NASA (Grant No. NAG-1-02070 and NCC-3-946), Office of Naval Research, Louisiana Board of Regents (Grant No. LEQSF(2001-04)-RD-B-09), and National Science Foundation (Grant No. NSF-DMR-0124765, NER, and CAREER award).

CM0491983